Effect of the Mineralogical Composition of Sandstones on the Wear of Mining Machinery Components

Andrzej N. Wieczorek *, Iwona Jonczy, Krzysztof Filipowicz, Mariusz Kuczaj, Arkadiusz Pawlikowski, Kamil Mucha, Anna Gerle

Posted Date: 27 May 2024

doi: 10.20944/preprints202405.1730.v1

Keywords: wear; sandstone; tribology; wear-resistant steels

Article

Effect of the Mineralogical Composition of Sandstones on the Wear of Mining Machinery Components

Andrzej N. Wieczorek [1]*, Iwona Jonczy [1], Krzysztof Filipowicz [1], Mariusz Kuczaj [1], Arkadiusz Pawlikowski [1], Kamil Mucha [2] and Anna Gerle [3]

[1] Silesian University of Technology, Faculty of Mining, Safety Engineering and Industrial Automation, Akademicka 2 Street, 44-100 Gliwice, Poland; andrzej.n.wieczorek@polsl.pl, iwona.jonczy@polsl.pl, krzysztof.filipowicz@polsl.pl, mariusz.kuczaj@polsl.pl, arkadiusz.pawlikowski@polsl.pl

[2] Faculty of Mechanical Engineering and Robotics, AGH University of Kraków, 30-059 Kraków, Poland; kmucha@agh.edu.pl,

[3] Łukasiewicz Research Network – Institute of Ceramics and Building Materials, Refractory Materials Division in Gliwice ul. Toszecka 99, 44-100 Gliwice, E-mail: a.gerle@icimb.pl

* Correspondence: andrzej.n.wieczorek@polsl.pl; Tel.: +48 322372124

Abstract: The paper provides and comments on the results of studies of the effect of sandstone-based abrasives and quartz sand alone on the wear of martensitic surfaces of wear-resistant steels. The wear process was examined on a ring-on-ring test rig seeking to determine the mass decrement parameter which characterised wear. The tests were conducted for three sandstone varieties: Carboniferous, Permian, and Cretaceous, and they made it possible to determine that the most intense process of deterioration of wear-resistant steels took place in the presence of quartz sand grain, while less intense wear was observed in the case of sandstone-based abrasives. The mass decrement values established in the presence of the sandstones in question did not differ significantly between individual sandstone varieties. Based on a surface damage analysis, the basic damage mechanism was found to be micro-scratching, however, with regard to the sandstones examined, it was also determined that individual grains could be pressed into surface irregularities, as well as that films of soft hematite cement developed in the Permian sandstone and that inclusions of carbonaceous matter were formed in the Carboniferous sandstone. With reference to the wear process observations, a wear model was described for the surface of the steels examined in the presence of sandstone-based abrasives.

Keywords: wear; sandstone; tribology; wear-resistant steels

1. Introduction

Considerable tribological wear is observed in mining machinery components working under harsh envi-ronmental conditions, which can be attributed to diverse causes, including the effect of aggressive abrasive materials. One of the main expectations held by companies which operate mining machines is the capacity to ensure their adequate availability. Excessive wear of machinery and equipment components is an issue typical of both underground and open cast mining. Consequently, the elements most prone to damage in-clude, for example, the liners of bins or buckets in excavators, power train caterpillars, or drive chains and drums of mining conveyors. The factors which link the aforementioned components are the presence of grain of different sandstone sorts in the zone where these elements work together and the widespread use of wear-resistant steel grades in their production.

This paper focuses on the overall body of problems pertaining to the operation of mining material handling machines used while dog headings are being driven [1,2], which represents a very complex range of sub-jects on account of the variety of issues and limitations experienced in the process, these being of geological and mining as well as technical nature. The work conducted in these headings is among the most labour- and time-intensive kinds. Dog headings, and the opening-

 doi:10.20944/preprints202405.1730.v1

out ones in particular, are currently driven in rocks characterised by very unfavourable parameters. What appears to be a relevant factor to this process is the type of rock-building minerals, since their hardness affects the rate of abrasion and wear of cutting tools. Additionally, the presence of specific concretions, such as those of spherosiderite, in rock banks causes intense sparking while mining operations are being performed, which poses a very serious threat in underground mines.

The equipment used for rock loosening and output haulage while driving tunnels or headings can be con-siderably diversified. It may comprise various types of conveyors, including scraper and belt conveyors, self-propelled machines moving on tyred wheels, excavators, roadheaders, loaders, or haulage cars [3]. In operation, individual components of these machines are exposed to factors which reinforce their surface damage [4,5]. Friction is one of the main causes of degradation of transport machinery components [6], yet an equally important degradation factor is the effect of abrasive material, the presence of which can signif-icantly intensify the processes of deterioration of the surfaces comprising a given tribological system (Figure 1). When combined, both these factors can induce an abrasive wear process. Abrasive wear can be defined as a process of deterioration and removal of material from the surface of a solid body, accompanied by a change in volume and the associated mass decrement [7–9]. An extreme case of abrasive wear can be a change in the structure and mechanical properties of elements engaged in friction, or even their physical degradation (Figure 2A).

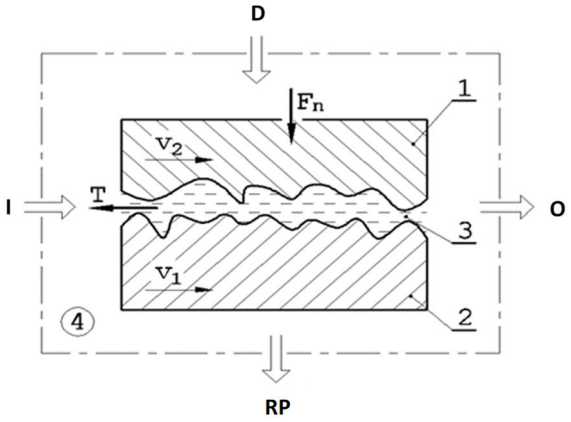

Figure 1. Tribological system [5]; designations: 1 – relative motion inducing element, 2 – element subject to kinematic forcing, 3 – intermediate layer, 4 – further surrounding, D – disturbances, Fn – load, I – pre-set input values (X), O – effective output values (Y), RP – residual processes, T – friction forces, 8 – v_1 and v_2 – surface velocities of elements 1 and 2.

A B

However, what proves to be more frequent is the effect of either dry (Figure 2B) or wet abrasive material (Figure 2C and 2D), which can cause significant material decrement precisely at the point of impact of this degra-dation factor. Material decrement in the surface layer can be due to such processes as micro-ridging, mi-cro-scratching, micro-fatigue, and micro-cracking [10]. In the case of

 doi:10.20944/preprints202405.1730.v1

abrasives composed of minerals char-acterised by considerable hardness, damage is typically attributable to micro-scratching or micro-ridging.

C D

Figure 2. Examples of the effect of environmental conditions observed while driving underground dog headings on elements of haulage machinery: A – example of critical damage to a conveyor track, B – conveyor track covered with dry rocky abrasive material, C – conveyor deck plate with visible scratches, D – chain links covered with a sticky mixture of rock and water; designations: 1 – deck plate abrasion.

The adverse effect of hard mineral abrasives on the surface of machine components has been extensively explored and discussed in the literature on the subject [10÷15]. However, clastic materials are often non-homogeneous and may contain materials of inherently diversified wear (abrasion) properties [16÷18]. Lawrowski [19] claims that the abrasive wear mechanism depends on the proportion between the hard-ness of the metal wearing away (HM) and the hardness of the abrasive (HA). Where HM/HA > 0.6, a less ag-gressive chemical-mechanical form of abrasion occurs, but where HM/HA < 0.6, edges of the abrasive grains cause surface micro-abrasion.

As aforementioned, the mineral composition of the rock mass in which dog headings are driven can be di-versified and variable along the entire driving section. This is precisely the situation presented and dis-cussed by Mucha [20] using an example of driving through a mass of rock and coal in order to develop an inclined ventilation drift in one of Polish coal mines. The geological cross-sections provided in Figure 3 formed layers of coal and sandstone (left-hand figure) and sandstone alone (right-hand figure).

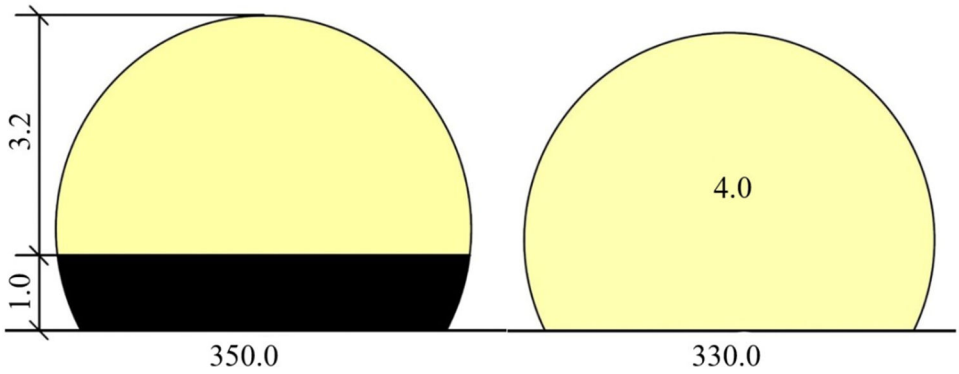

Figure 3. Examples of geological cross-sections of an underground dog heading; designations: yellow – sandstone, black – coal (based on [20]).

It is common that underground headings are driven in sandstone-containing rock formations [3]. Sandstones [21÷24] represent a group of clastic rocks which – on account of the grain size of the clastic material – are classified as psammitic. There are generally two groups of components found in the structure of sandstones: allogenic minerals, forming what is referred to as the grain skeleton, and authigenic minerals, contained in the binding matter commonly known as cement. There is also a separate group known as the matrix, comprising allogenic grains of a size below the lower limit of

 doi:10.20944/preprints202405.1730.v1

the fraction which represents the grain skeleton. The allogenic grains include weathering-resistant minerals derived from the comminution of older rocks, and these are primarily quartz, feldspar (most commonly represented by orthoclase, albite, and oligoclase), mica (mainly muscovite, less commonly biotite), and heavy minerals such as zircon and garnets. The authigenic minerals, on the other hand, are formed where sediment develops, during either sedimentation or diagenesis. These include opal, chalcedony, carbonates, clayey minerals, iron oxides and hydroxides.

Sandstones can be classified according to diverse criteria [25]. Considering the grain size diversity of the grain skeleton, sandstones can be broken down into coarse-grained (1–2 mm), medium-grained (0.5–1 mm), fine-grained (0.25–0.5 mm), and very fine-grained (0.10–0.25 mm) sandstones. The sandstone varieties depending on the mineralogical composition are either monomineral, quartz being their main component, or polymineral. As per Folk's [26] classification, the polymineral sandstones include arkose (containing numerous feldspar grains besides quartz) and greywacke sandstones rich in rock clast and clayey minerals. According to Petitjohn [27], on the other hand, the breakdown of sandstones should also be based on the fraction of matrix, besides the mineralogical composition. Such an assumption leads to the division into arenytes (containing up to 15% of matrix by vol.) and wackes (containing 15–75% of matrix by vol.).

Sandstones can also be subdivided on account of the mineralogical composition of cement, which basically affects their physical and mechanical properties, and so there can be siliceous, calcareous, clayey, ferruginous, and other sandstones. The mineralogical composition of cement determines the sandstone colour, which also plays an important role, especially in construction stone production. Therefore, for instance, one can distinguish between white (Cretaceous), red (Permian), pink (Triassic), and green (Cretaceous) sandstones.

There is a relatively plentiful body of research on the mechanical properties of sandstones. These characteristics, including fatigue strength, susceptibility to cracking, and axial load behaviour, as well as the failure mechanisms of sandstones have been studied by numerous authors, some of whom are: Z. Song et al. [28], Bagde and Petroš [29–31], Song, H et al. [32], Cai et al. [33], Y. Zhao et al. [34], Vaneghi et al. [35], Yang et al. [36–38], G. Zhao et al. [39], Liu et al. [40], Ray et al. [41], Feng et al. [42], Figarska-Warchoł et al. [43], and Li et al. [44]. The abrasiveness of sandstones, on the other hand, has been addressed in papers [45÷55].

In order to counteract the excessive abrasive wear of working surfaces in the machinery and equipment operated while driving dog headings and tunnels, typically caused by the effect of rocks, including sandstones, wear-resistant steels are used in production. These steel grades are classified as martensitic, weldable, resistant to abrasive wear, and characterised by very high strength parameters [56÷58]. Their anti-wear properties have been examined relatively extensively in terms of the potential impact of quartz grains or rock mixtures forming different variations of mineral aggregates [15÷17,57÷64].

In their studies released to date the authors have analysed the effects of quartz sand [65], coal [66], siltstones [67] as well as their mixtures with quartz sand [68] on the wear of wear-resistant steels. This body of research has allowed them to conclude that the content of low-hardness minerals in the rock material can exert a fundamental impact on the underlying damage mechanism of the steel grades in question, thereby determining the intensity of their wear. The role of rocks such as siltstone or coal may consist in changing the three-body form of abrasive wear to the less intense two-body form of wear of the grains embedded in the material wearing away. Furthermore, clayey minerals and coal show a tendency to being pressed into surface irregularities and can immobilise steel wear products. Consequently, in the processes of abrasive wear of martensitic steels in the presence of sandstones composed, as aforementioned, primarily of quartz and cement, the damage mechanism at play may not necessarily be solely the one typical of hard grain, such as quartz. Based on that observation, Wieczorek et al. [69] proposed a wear model for mixtures of hard grains and soft phases, dedicated to elements of tunnelling machinery. In the case of sandstones, specific wear mechanisms as well as the interactions between wear processes can be complex [70] and conditioned by the components comprising a given tribological system [71÷73].

The primary objectives of the research addressed in this paper were:

 doi:10.20944/preprints202405.1730.v1

– s

In order to achieve the objectives of their research, the authors focused on identifying the mineralogical composition of the sandstones under consideration. Additionally, they compared the results obtained in the studies they had conducted with the results pertaining to the effect of quartz sand grains. With reference to the preliminary research, it should also be concluded that the literature on the subject lacks analyses of the impact of the mineralogical composition of sandstones on the damage mechanisms of wear-resistant steels, which makes the research addressed in this paper and its results novel, given the current state of knowledge in the field of wear processes.

2. Experimental Details

In pursuit of the main research objectives, the following studies were conducted:

– mineralogical and chemical identification of the analysed abrasive material based on microscopic observations of thin plates using a scanning electron microscope, as well as analysis of chemical composition by X-ray fluorescence (XRF),
– wear testing of wear-resistant steels in the presence of comminuted sandstone grains and quartz sand,
– identification of the surface damage mechanisms observed in the samples based on scanning microscopy observations and EDS analysis.
– Besides quartz sand, three sandstone types were used in the studies:
– Carboniferous sandstone obtained from the Piast-Ziemowit hard coal mine in Bieruń,
– Permian ferruginous sandstone from the Lower Silesian deposits found in the district of Kłodzko,
– sandstone from the bottom Godulian strata extracted in the town of Wisła, dating back to the Upper Cretaceous.

Do badań wykorzystano, oprócz piasku kwarcowego, 3 rodzaje piaskowców:

– piaskowiec karboński z wyrobiska KWK Piast-Ziemowit w Bieruniu,
– piaskowiec żelazisty datowany na perm pochodzący dolnośląskich złóż w powiecie kłodzkim,
– piaskowiec z dolnych warstw godulskich w Wiśle, datowany na górną kredę.

Thin plates of material were used to perform transmitted light microscopy observations by means of the OPTA-TECH LAB-40 HAL polarised light diagnostic microscope featuring an image analyser.

In order to determine the chemical composition of the sandstones by X-ray fluorescence (XRF) in line with the EN ISO 12677: 2011 standard, the samples were ground to a grain size of less than 63 μm using a tung-sten carbide-lined mill. The samples were dried, and then the relevant loss on ignition was determined at the temperature of 1,025°C. Roasted to a constant mass, the samples were melted using an off-the-shelf mixture of lithium tetraborate, lithium metaborate, and lithium bromide (66.67%, 32.83%, and 0.5%) of a flux purity suitable for XRF (from Spex). The sample-to-flux weight ratio was 1:9. Thus prepared, the sam-ples were measured using the PANalytical MagiX PW2424 spectrometer calibrated with a series of certified reference materials, i.e. JRRM 121-135, JRRM 201-210, JRRM 301-310 (Technical Association of Refractories, Japan).

The surface of the steel as well as sandstone samples were subject to observations at the fracture, conducted using the SEM AXIA ChemiSEM scanning electron microscope from ThermoFisher Scientific with a fully integrated EDS spectrometer using secondary electron (SE) detection at an accelerating voltage of 15 kV and magnification ranging from x50 to x2,000. The chemical composition in micro-areas was subject to a qual-itative analysis by energy dispersive X-ray spectroscopy (EDS) at an accelerating voltage of 15 kV. For test-ing purposes, the sandstone samples were sputtered with gold using the SPT-20 COXEM sputter coater, while surface texture examinations were performed using the Profilm3D optical profilometer from Filmet-rics Inc. (San Diego, CA, USA).

The tribological test samples were made from a wear-resistant steel with the trade name of RAEX400. The main material data of the steel subject to the tests have been provided in Table 1, while its chemical compo-sition – in Table 2. Detailed information on the steel used in the studies can be found in papers [68,69]. The surface profilogram of the RAEX400 steel has been shown in Figure 5.

 doi:10.20944/preprints202405.1730.v1

The abrasive wear tests were conducted at a ring-on-ring type test rig (Figure 6A,B). One of the characteristics of the test [68,69] was the constant presence of comminuted grains of sand or the sandstones ana-lysed. Two ring-shaped samples of the RAEX400 steel (Figure 6C) were fixed in the upper and lower holders of the test rig so as to arrange them parallel to each other and to prevent them from moving in the holders.

Table 1. Mechanical properties of the steel tested.

Mechanical Properties	Tensile Strength TS, MPa	Elongation A, %	Minimum temperature for which the steel impact strength V is 30 J, °C	Hardness, HB
RAEX400	1250	10	-40	383÷403

Table 2. Chemical composition of the tested steel [mass%].

C	Mn	Si	S	P	Ni	Cr	Mo	B	Nb
0.288	1.14	0.436	0.0124	0.0042	0.0782	0.457	0.122	0.0063	<0.004

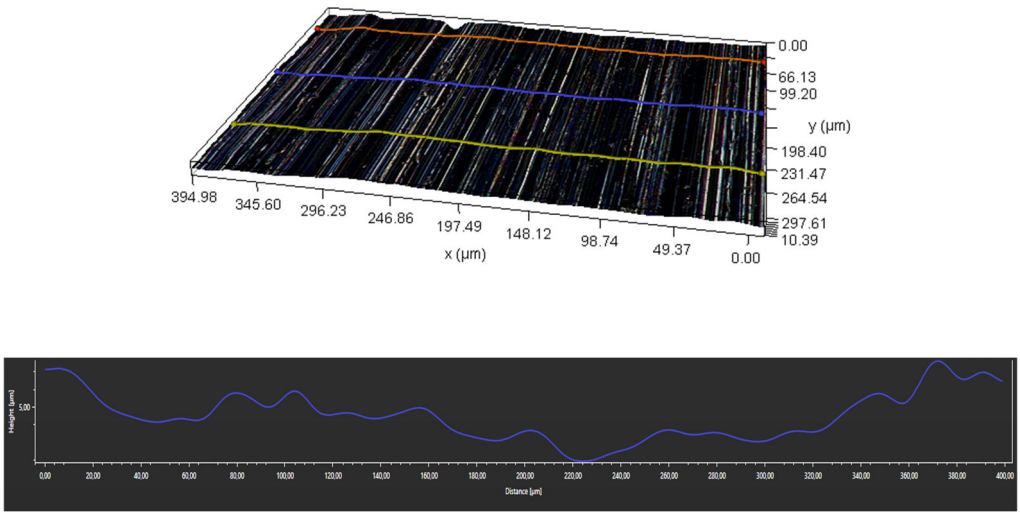

Figure 4. Surface profilogram of the RAEX400 steel sample prior to wear testing.

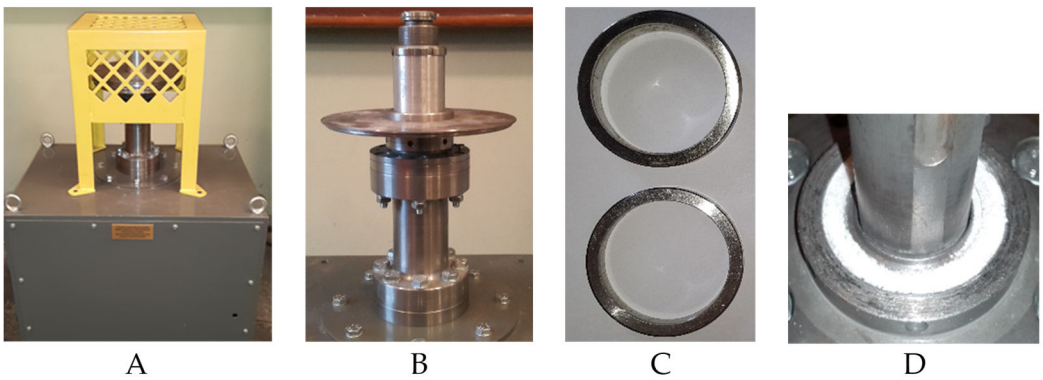

Figure 5. Tribotester; A – test rig, B – testing head, C – sample, D – bottom holder with abrasive material.

 doi:10.20944/preprints202405.1730.v1

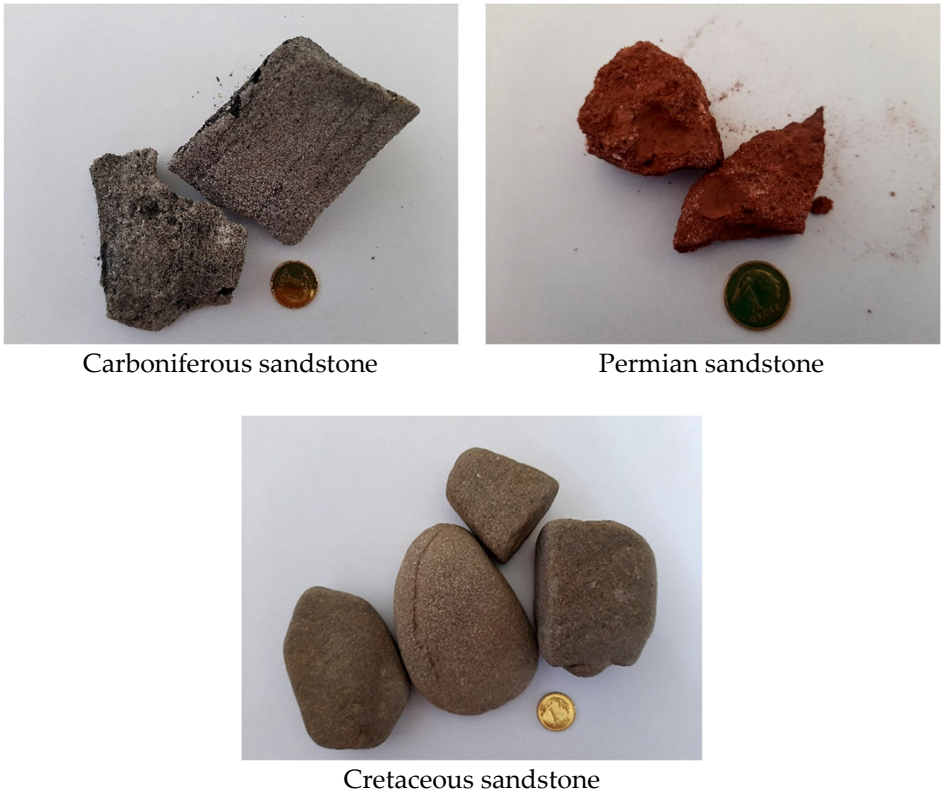

Figure 6. Samples of the sandstones subject to the tests.

Prior to the testing, the abrasive material subject to the tests was ground to a grain size of less than 100 μm and placed in an amount corresponding to 1 cm3 between the faces of the samples. While exerting its im-pact on the steel surfaces, the abrasive continued to grind out. The samples were cleaned and weighed be-fore and after a 10-minute wear cycle to determine their mass decrement, while fresh abrasive was added between the test samples before the start of each cycle. For each abrasive variant and each load value, three test series were performed, each consisting of eight wear cycles. The parameters characterising the wear tests have been provided in Table 3.

Table 3. Main parameters of the wear tests.

Parameter	Value			
Contact surface area S, mm²	785.3			
Compressing stress σ, MPa for				
Quartz sand	0.031	0.062	0.094	0.125
Carboniferous sandstone			0.094	0.125
Permian sandstone	0.031	0.062	0.094	0.125
Cretaceous sandstone			0.094	0.125
Tests duration, min	8 × 10			
Sliding distance, m	1390			
Rotational speed of the moving sample, RPM	149.1			
Average linear speed of the moving sample, m/s	0.29			
Number of test repetitions for each variant	3			
Outside diameter of the sample	Ø55h8			
Inside diameter of the sample	Ø45H7			
Sample width (B)	for upper lid B = 10 mm, for lower lid B = 6 mm			

 doi:10.20944/preprints202405.1730.v1

Based on the mass measurements conducted after the 10-minute wear cycles, the mass decrement of sam-ple uM was determined according to formula (1):

$$W_M = \left(M_{\mathrm{BS\_End}} - M_{\mathrm{BS\_Start}}\right) + \left(M_{\mathrm{US\_End}} - M_{\mathrm{US\_Start}}\right) , \quad (1)$$

where: W_M – weight loss of the sample in g, M_{BS_Start} – mass of the bottom sample before the test in g, M_{BS_End} – end mass of the bottom sample in g, M_{US_Start} – mass of the upper sample before the test in g, M_{US_End} – end mass of the upper sample in g.

Measurement uncertainty was determined using Student's T-method for confidence level equal to 0.95 and number of tests n = 3. The relative measurement uncertainty was less than 3% for all the cases considered.

 doi:10.20944/preprints202405.1730.v1

3. Results

3.1. Identification Tests

Carboniferous sandstone (Figure 4A) is characterised by its grey colour, medium-grained texture, and low de-gree of sorting. The sandstone texture is compact, typically chaotic, only locally with directional texture marked by the presence of fine-grained parallel layers of carbonaceous matter. In a sample comprising chunks of material, sandstone reacts with HCl when exposed to cold, which implies that there is calcite (CaCO3) in the mineralogical composition of the cement, and moreover, a distinct odour of mortar is re-leased when the rock comes into contact with water, which, in turn, indicates the presence of clayey miner-als.

Permian sandstone (Figure 4B) is red in colour, which indicates the presence of iron oxides, mainly hematite (Fe_2O_3), in the mineralogical composition of the cement. The structure of this sandstone is medium-grained with a low degree of sorting. Its texture is chaotic, typically compact, yet fine pores can be observed locally on the rock surface. This sandstone is also brittle.

Cretaceous sandstone (Figure 4C) displays a light grey colour and a fine-grained texture with a high degree of sorting of the clastic material. The texture of the sandstone is compact and chaotic. Macroscopic examina-tions reveal that, besides quartz, there are lamellae of muscovite with a characteristic pearly lustre in the mineralogical composition of the sandstone clast.

In order to identify the structure and mineralogical composition of the sandstones under consideration, transmitted light microscopic observations were conducted using a scanning electron microscope. Figures 7 and 8 are microphotographs of the grain surface and microstructure of the Carboniferous sandstone, Figures 9 and 10 show the Permian sandstone, while Figures 11 and 12 – the Cretaceous sandstone.

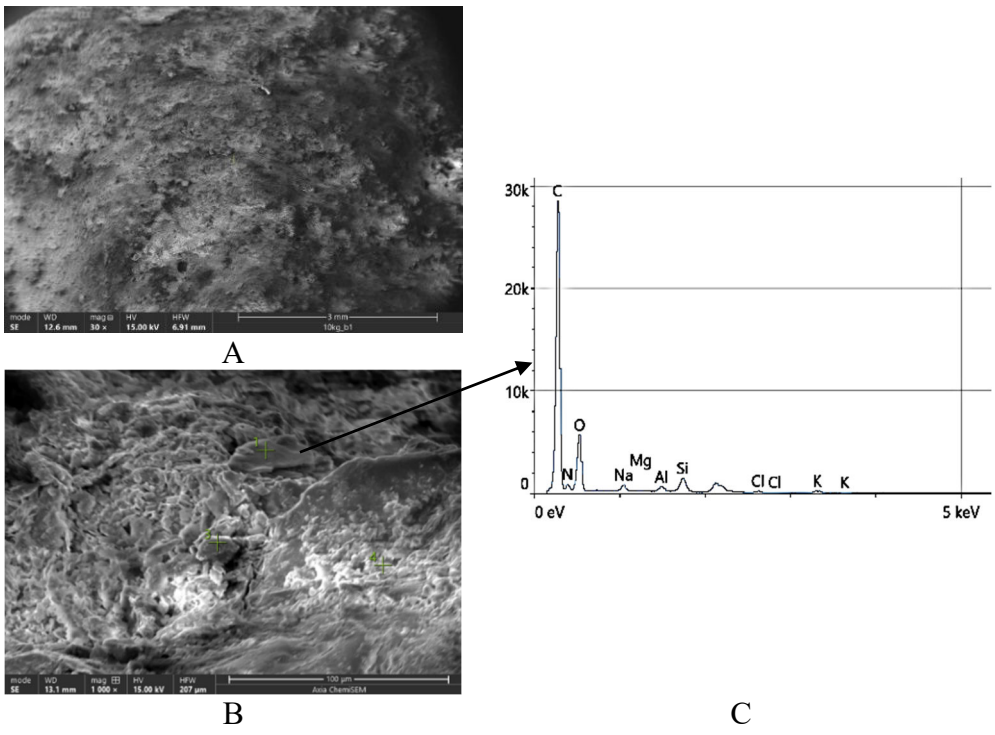

Figure 7. Carboniferous sandstone surface: A – microscopic view (x30, SEM), B – microscopic view (x1,000, SEM); C – EDS analysis results for item 1.

 doi:10.20944/preprints202405.1730.v1

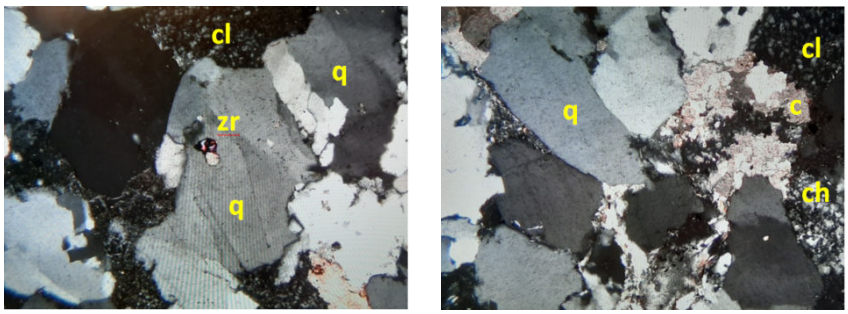

Figure 8. Microphotograph of Carboniferous sandstone (in transmitted light, crossed polarisers, x100); designations: q – quartz, cl – clayey minerals; c – carbonates, ch – chalcedony, zr – zirconium.

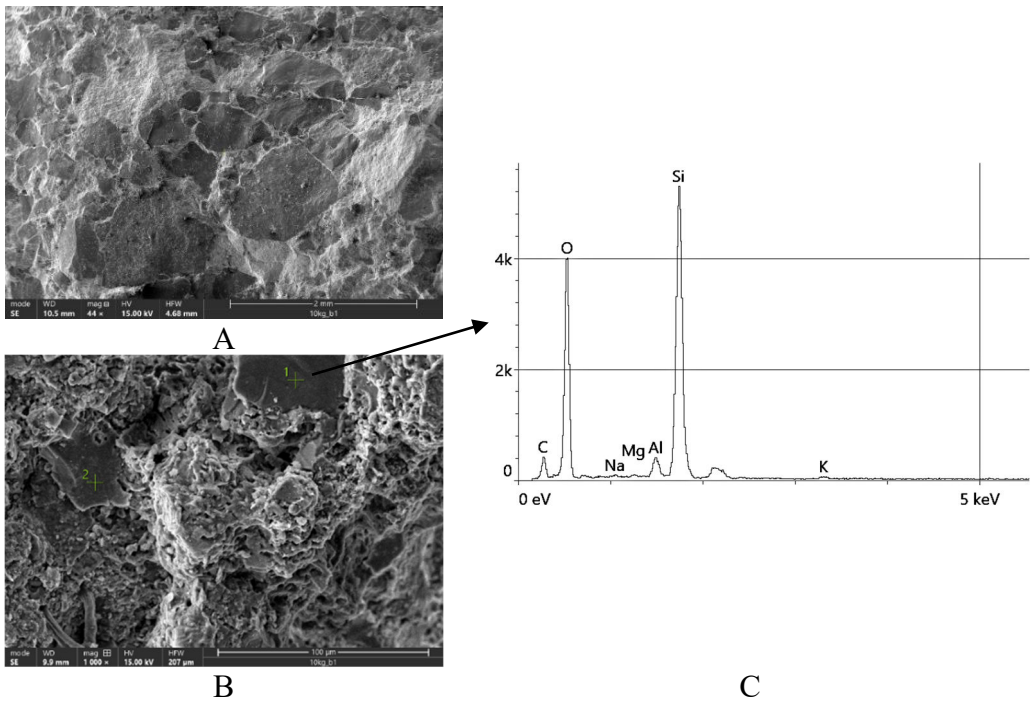

Figure 9. Permian sandstone surface: A – microscopic view (x44, SEM), B – microscopic view (x1,000, SEM); C – EDS analysis results for item 1.

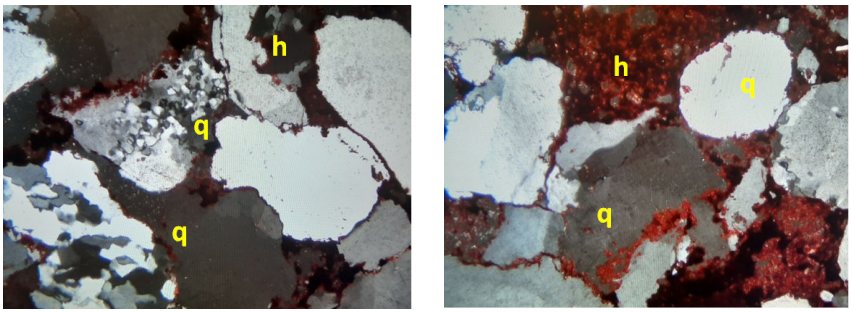

Figure 10. Microphotograph of Permian sandstone (in transmitted light, crossed polarisers, x100); designations: q – quartz, h – hematite.

 doi:10.20944/preprints202405.1730.v1

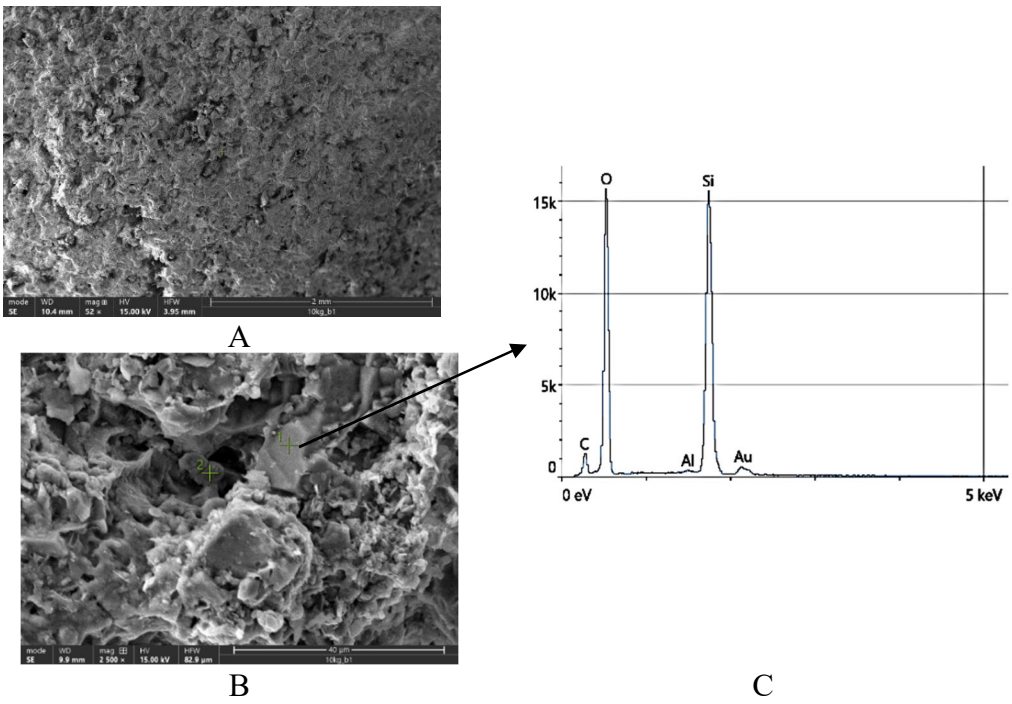

Figure 11. Cretaceous sandstone surface: A – microscopic view (x44, SEM), B – microscopic view (x1,000, SEM); C – EDS analysis results for item 1.

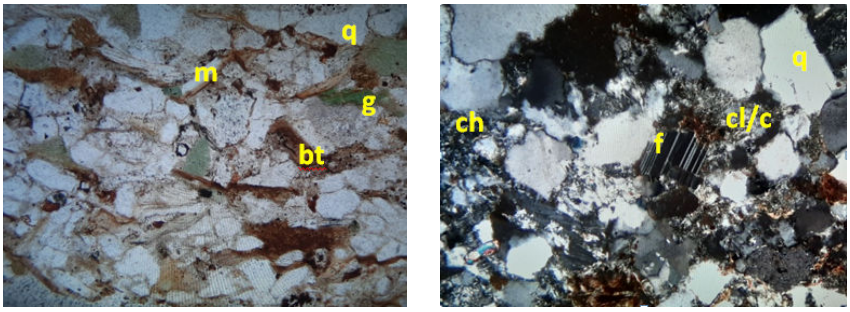

Figure 12. Microphotograph of Cretaceous sandstone (in transmitted light; left – parallel polarisers, right – crossed polarisers, x100); designations: q – quartz, cl – clayey minerals; c – carbonates, f – feldspars, ch – chalced-ony, m – muscovite; bt – biotite; g – glaukonite.

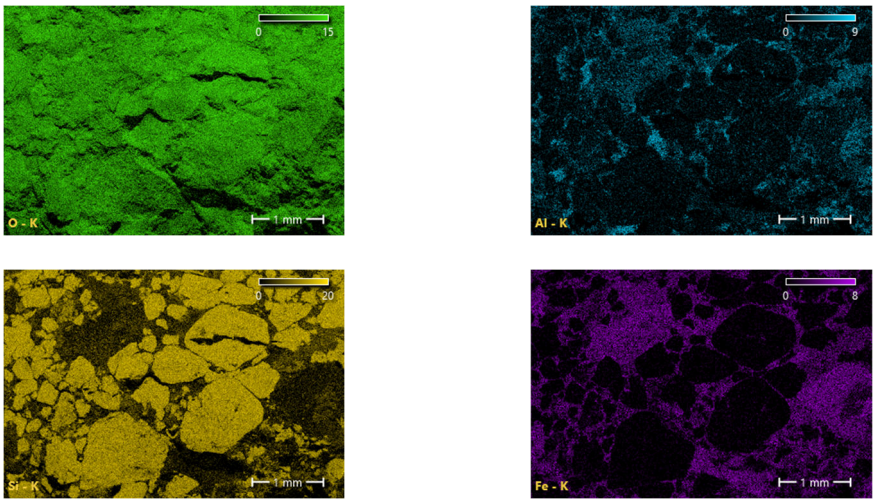

Figure 13. Element distribution on the Permian sandstone surface (elements designated in figures).

 doi:10.20944/preprints202405.1730.v1

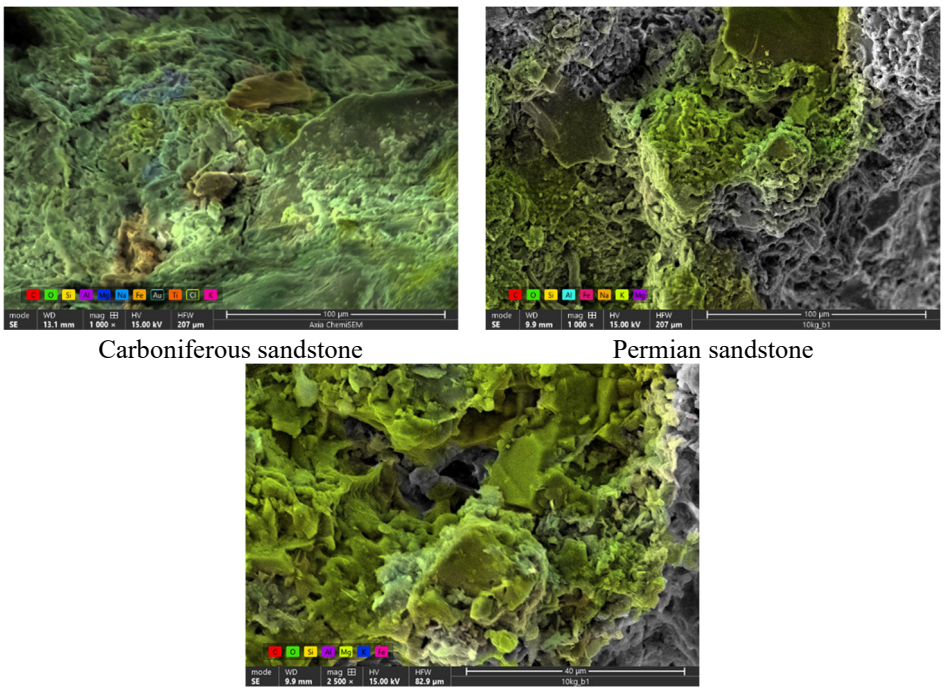

Figure 14. Element maps identified for the sandstones studied.

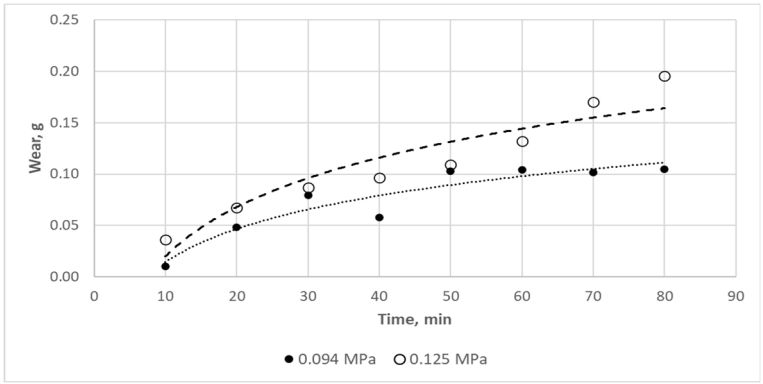

Carboniferous sandstone

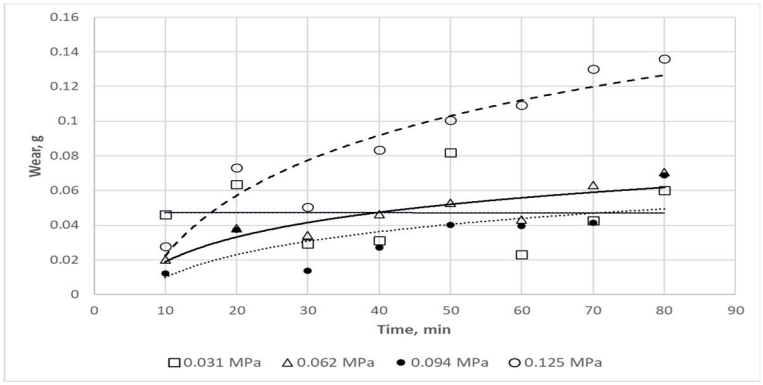

Permian sandstone

 doi:10.20944/preprints202405.1730.v1

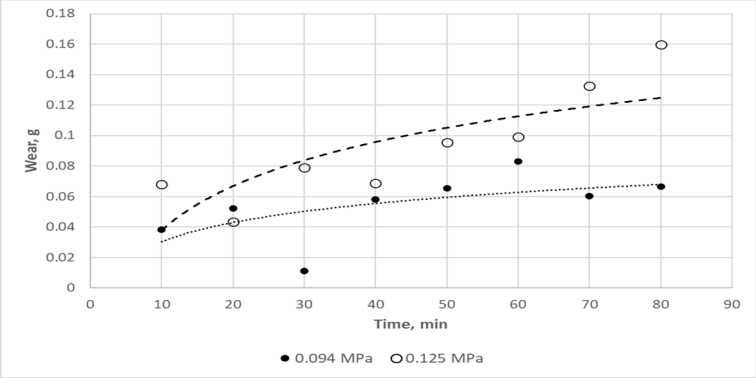

Cretaceous sandstone

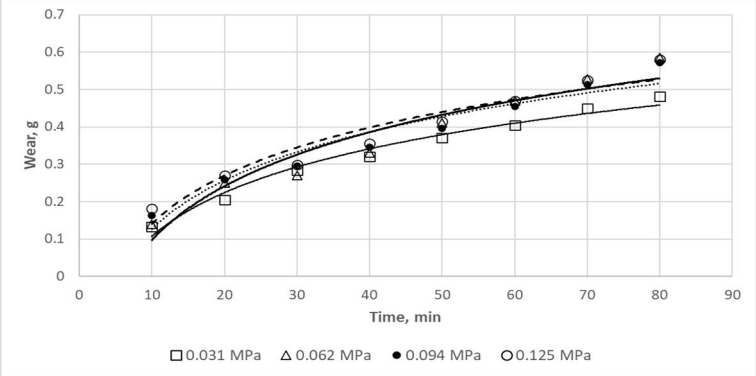

Sand quartz

Figure 15. Behaviour of mass decrement (W_M) of wear-resistant steel in a function of testing time established for the sandstone varieties and quartz sand examined.

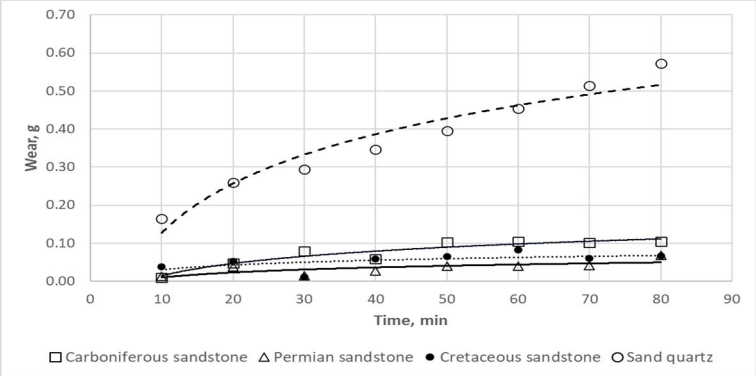

0.094 MPa

Having performed the microscopic observations and spot EDS measurements, the authors also established the surface distribution of elements. A sample distribution obtained for the Permian sandstone has been shown in Figure 13) and the elements were mapped for the sandstones studied (Figure 14). Figure 15 shows the surface of the quartz sand used in the studies. Additionally, the sandstones subject to testing were also an-alysed for chemical composition (Table 4).

3.2. Wear Tests

Figure 15 illustrates the behaviour of mass decrement in a function of testing time for the sandstone varieties and quartz sand examined, while Figure 16 provides a comparison of wear curves for the sandstone varieties in question.

The wear test results obtained imply the following findings:

– the greatest wear was observed for homogeneous hard mineral abrasives (quartz sand),
– all the wear values obtained for the wear-resistant steel in the presence of quartz sand and for all load values are very similar,

 doi:10.20944/preprints202405.1730.v1

– the differences in the mass decrement caused by the presence of Permian, Carboniferous, and Creta-ceous sandstone are inconsiderable and cannot be graded in terms of the intensity of their effect on the wear-resistant steel.

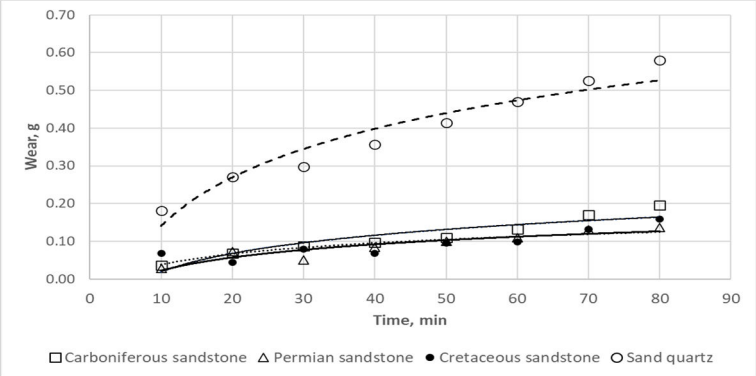

0.125 MPa

Figure 16. Comparison of curves of mass decrement (WM) of wear-resistant steel for the sandstone varieties examined: A – for 0.094 MPa of load, B – for 0.125 MPa of load.

Table 4. Results of analysis of chemical composition of studied sandstones.

Minerał, %	Carboniferous sandstone	Permian sandstone	Cretaceous sandstone
SiO_2	88.53 ± 2.21	80.27 ± 2.01	83.14 ± 2.08
Al_2O_3	3.83 ± 0.19	5.09 ± 0.25	8.06 ± 0.40
Fe_2O_3	0.35 ± 0.17	11.81 ± 0.59	2.88 ± 0.14
TiO_2	0.17 ± 0.09	0.23 ± 0.12	0.37 ± 0.19
MnO	0.02 ± 0.01	0.01 ± 0.01	0.04 ± 0.02
CaO	0.62 ± 0.31	0.03 ± 0.02	0.25 ± 0.12
MgO	0.49 ± 0.25	0.09 ± 0.05	0.66 ± 0.33
Na_2O	0.53 ± 0.26	0.01 ± 0.01	1.63 ± 0.16
K_2O	0.67 ± 0.33	0.43 ± 0.22	1.41 ± 0.14
P_2O_5	0.01 ± 0.01	0.09 ± 0.04	0.07 ± 0.03
strata prażenia *	4.73 ± 0.47	2.42 ± 0.24	1.86 ± 0.19
* strata prażenia wyznaczona w temp. 1025 °C			

3.3. Surface Analysis After Wear Tests

Once the wear tests had been completed, the next stage in the research consisted in assessing the effects of the abrasive materials on the surface of the steel samples tested. For this purpose, microscopic observations of the steel surfaces were performed by optical profilometry and scanning electron microscopy. What could be found on the surface of all the steel samples tested in the presence of three types of sandstone and quartz sand was the wear forms typical of hard abrasives, forming scratches whose presence was caused by the impact of quartz grains. This can be clearly seen in the profilograms provided in Figure 17.

 doi:10.20944/preprints202405.1730.v1

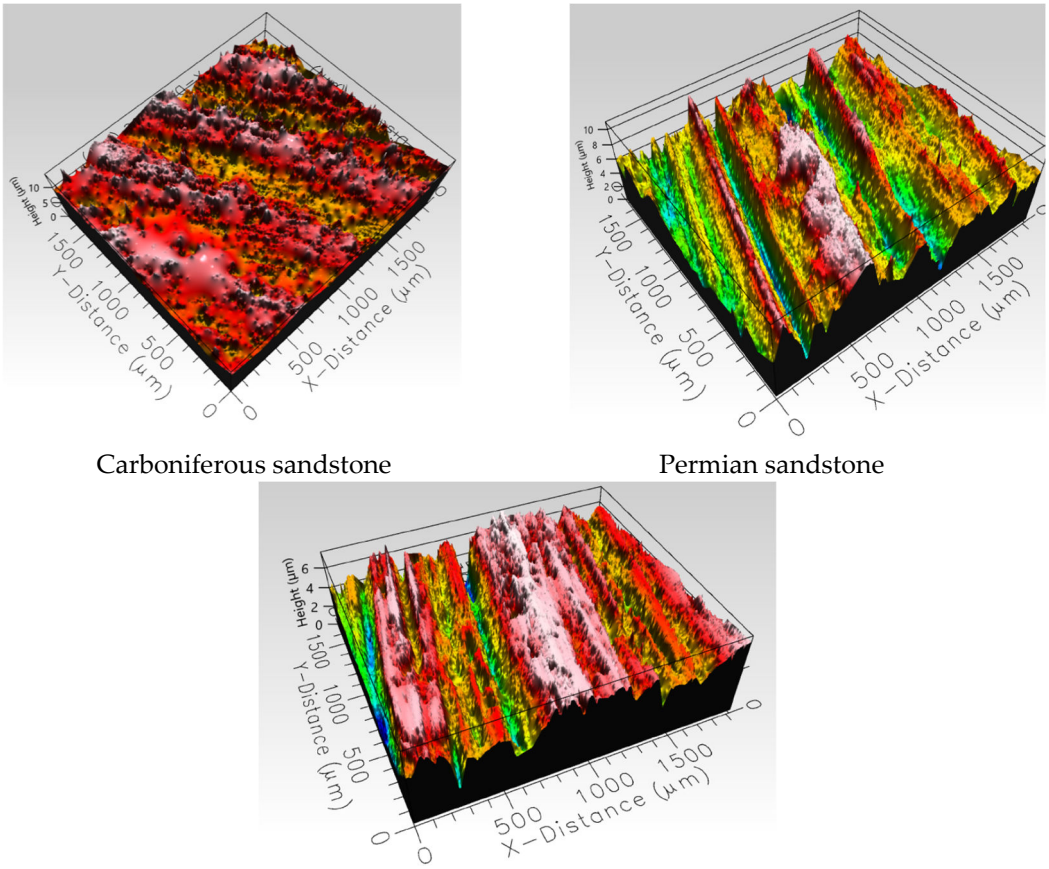

Carboniferous sandstone

Permian sandstone

Cretaceous sandstone

Figure 17. Profilograms of the surface of wear-resistant steel wearing away in the presence of sandstone clast, as de-termined for a load of 0.125 MPa.

What these profilograms also demonstrate for all the three sandstone varieties studied is surface zones characterised by plastic minerals, forming the sandstone cement, having been partially pressed into scratches which developed earlier. However, the images of the surface of the wear-resistant steel wearing away in the presence of sandstone grains (Figure 18÷20) reveal far more forms of damage.

In numerous cases of the steel tested in the presence of the Carboniferous sandstone-based abrasive, it was observed that, due to the wear caused by the presence of grains between mating surfaces, the carbonaceous substance had been pressed into the scratches formed on the surface, but finer crumbs thereof were also found to have mixed with some harder components of the abrasive material showing on the steel surface (Figure 18). Visible in this figure are also quartz grains embedded in the surface either directly or via a layer of coal previously pressed in.

The microphotographs of the steel samples exposed to the impact of the Permian sandstone-based abrasive clearly show that scratches were filled by hematite (Fe2O3), which is the main component of the sandstone cement (Figure 19). The remaining, non-pressed part of the haematite-rich cement was subjected to the effect of friction. Affected by load and relative surface motion, the abrasive material displayed a tendency to aggre-gate into larger lumps, mostly typically to be found in surface chipping areas.

 doi:10.20944/preprints202405.1730.v1

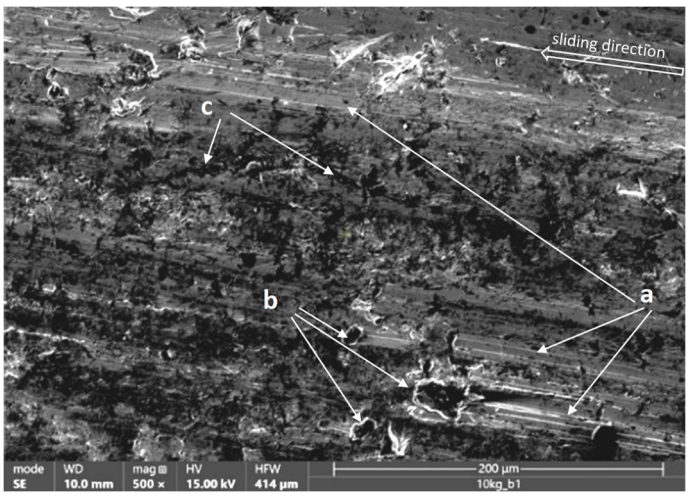

A

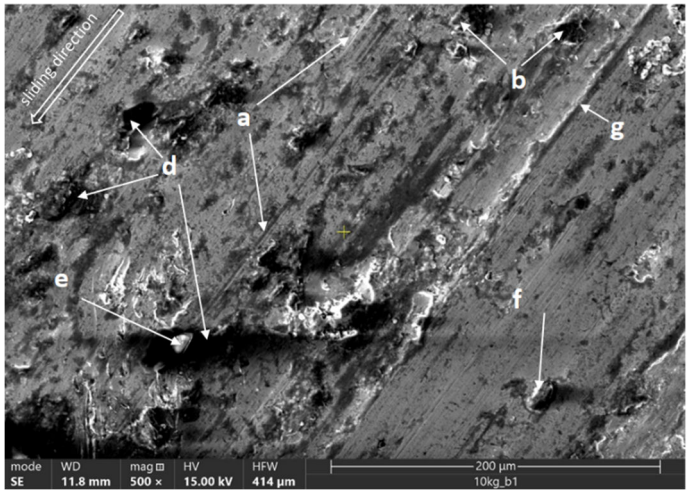

B

Figure 18. Surface of wear-resistant steel wearing away under a load of 0.125 MPa in the presence of Carboniferous sandstone clast: a – scratches, b – clasts of carbonaceous matter, c – coal-filled surface cracks, d – carbona-ceous films, e – quartz grain embedded in carbonaceous film, f – quartz grain embedded in surface, g – groove.

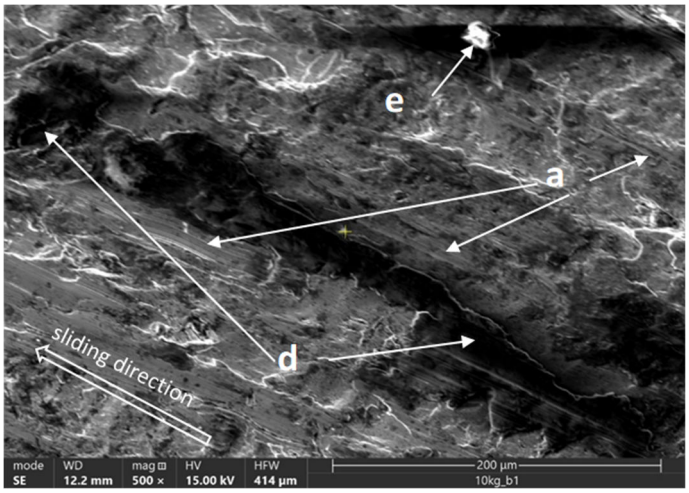

Figure 19. Surface of wear-resistant steel wearing away under a load of 0.125 MPa in the presence of Permian sand-stone clast: a – scratches, d – hematite films, e – quartz grain embedded in hematite film.

 doi:10.20944/preprints202405.1730.v1

The surface of the steel samples exposed to the effect of the Cretaceous sandstone abrasive has shown rela-tively the greatest signs of wear. Clearly visible are the scratches created by the abrasive action of quartz (Figure 20) as well as the crushed quartz grains embedded in the steel surface, surrounded by clusters of min-eral cement.

Figure 21 shows examples of the damage which the wear-resistant steel surface sustained following the wear tests in the presence of quartz sand. The effect of the grain, as observed on the surface of the test samples, was damage in the form of numerous extensive scratches. Between these scratches, patches of smoothed surface or with small pinpoint cavities can be seen. No embedded quartz sand grains or any films of pressed-in mineral grain were found on the surface of the test samples.

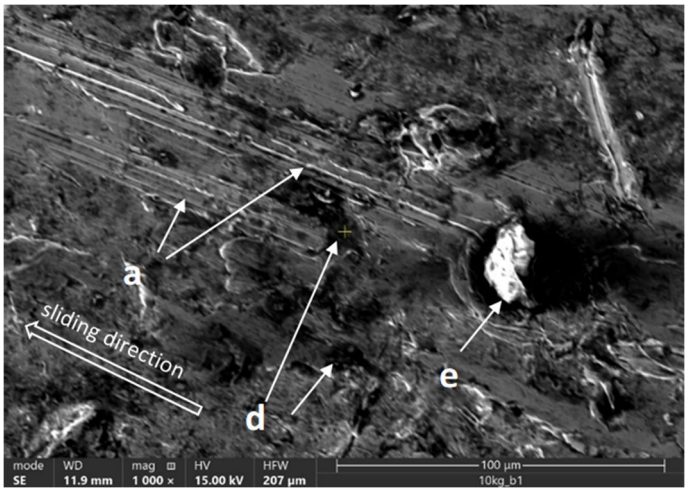

Figure 20. Surface of wear-resistant steel wearing away under a load of 0.125 MPa in the presence of Cretaceous sandstone clast: a – scratches, d – carbonaceous films, e – quartz grain embedded in carbonaceous film.

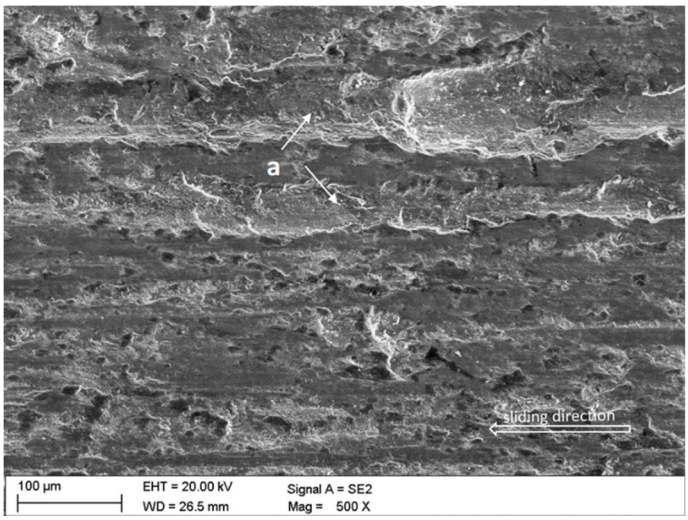

Figure 21. Surface of wear-resistant steel wearing away under a load of 0.125 MPa in the presence of quartz sand grain: a – scratches.

4. Discussion

Quartz is the primary mineral forming the grain skeleton of all the sandstone varieties examined. Quartz grains are characterised by diversified size ranging between 0.1 mm and 1 mm as well as varying degree of roundness. Alongside rounded-edge samples, sharp-edged grains could also be discerned, especially in the Cretaceous sandstone. With the polarisers arranged in parallel, the quartz grains appear colourless with weakly positive relief; their surface is predominantly scratched and

 doi:10.20944/preprints202405.1730.v1

covered with a lattice of irregular cracks. With the crossed polarisers in use, first-order grey interference colours characteristic of quartz are visible, but one can also observe some optical anomalies caused by the dynamic deformations to the quartz lattice. The foregoing causes wavy light extinction, which means that the surface of individual grains is not extinguished uniformly, but rather in a fragmented fashion instead, which manifests itself as locally ex-tinct patches within the grain.

Mica can be found primarily in the Cretaceous sandstone, with incidental occurrences in the Carboniferous and Permian sandstone. This group is represented by well-preserved grains of muscovite, forming elon-gated idiomorphic shapes, often twisted upon contact with other minerals. With the parallel polarisers in use, muscovite is colourless and non-pleochroic, showing distinctive unidirectional cleavage. With the crossed polarisers, second- and even third-order interference colours are marked, characteristic of musco-vite. In addition to muscovite, biotite is found in the Cretaceous sandstone. Biotite grains are highly weath-ered, typically with jagged edges, while well-preserved idiomorphic crystals can rarely be observed. With the polarisers arranged in parallel, biotite appears to be characterised by a brown colour and pronounced pleochroism, with unidirectional cleavage visible on the grain surface. With the crossed polarisers in use, biotite shows simple light dimming and second-order interference colours.

The feldspar group is represented mainly by plagioclases, identified in all the sandstones studied. They form fine grains showing grey interference colours and characteristic polysynthetic twinning. Heavy min-erals were mainly observed in the Carboniferous sandstone, And these included zircon, found to have formed well-rounded colourless grains with characteristic black pleochroic rims. With the polarisers crossed, zircon shows fourth-order interference colours.

The binding matter in the Carboniferous and Cretaceous sandstone represents the porous type, while it is primary in nature in the Permian sandstone. It is a mixed cement type, and no matrix type cement was ob-served. In the Carboniferous sandstone, chalcedony, clayey minerals, and carbonate-based minerals were found among the cement components. Chalcedony forms microcrystalline aggregates whose individual grains show optical characteristics similar to those of quartz: they are colourless and non-pleochroic, with zero or weakly positive relief, showing no cleavage. With the crossed polarisers in use, they are character-ised by grey interference colours of the first order. Clayey minerals form microcrystalline aggregates with dark grey interference colours. Carbonates are colourless with variable relief, and with the crossed polaris-ers in use, they show fourth-order interference colours.

The main component of the Permian sandstone's cement is oxidised iron compounds, represented primar-ily by hematite with a characteristic red colour. In the Cretaceous sandstone, as in the Carboniferous one, the cement is of mixed clay-carbonate-silica type, but what is particularly noteworthy about it is the frac-tion of glauconite, belonging to the group of clayey minerals. The most characteristic feature of glauconite is its green colour observed in the microscopic image with the polarisers in the parallel arrangement.

In the Carboniferous sandstone, the texture was confirmed to be compact (Figure 6A), and furthermore, clasts of carbonaceous matter were found among the sandstone's structural components (Figure 7). The micropho-tographs of the Permian sandstone clearly show the presence of ferruginous cement which, on account of the clast-to-cement ratio, is primary in nature (Figure 9). On the other hand, among the components of the clastic material, well-preserved irregular quartz grains could be observed (Figure 10). The microscopic analy-sis of the surface of the Cretaceous sandstone revealed micropores which were not discernible in the mac-roscopic observations (Figure 11). The quartz grains were also found to be characterised by a much smaller size compared to the quartz forming the Carboniferous and Permian sandstone, which had already been established during the macroscopic observations, implying that the structure of the Cretaceous sandstone should be categorised as fine-grained (Figure 12).

The analysis of the chemical composition of the sandstones examined has shown that their dominant component is silica (SiO_2), whose content in the Carboniferous and Cretaceous sandstone is 88.53% and 83.14%, respectively, while the smallest content of this component has been identified

 doi:10.20944/preprints202405.1730.v1

in the Permian sandstone – 80.27%. Silica occurs alongside the oxides of aluminium (Carboniferous sandstone – 3.83%, Permian sandstone – 5.09%, Cretaceous sandstone – 8.06%), iron (the most found in the Permian sand-stone (11.81%) and the least (0.35%) – in the Carboniferous sandstone), and potassium (Carboniferous sandstone – 0.67%, Permian sandstone – 0.43%, Cretaceous sandstone – 1.41%). The other oxides are pre-sent in smaller amounts, their content not exceeding 1%. The loss on ignition implies that admixtures of organic matter are present in the sandstone composition, found in the largest content in the Carboniferous sandstone (4.73%).

In their previous papers [4,64–68], the authors have demonstrated that the fraction of quartz, or possibly also of the SiO_2 + Al_2O_3 complex, in abrasive mixtures has a decisive impact on the rate of wear of wear-resistant steels. The study addressed in this paper also served to establish a relation between the wear rate and the fraction of quartz (SiO_2) expressed in per cent (Figure 22).

Figure 22 shows that, within the range of 80÷88% of the SiO_2 content, the increase in mass decrement is rela-tively small, and not until the quartz content nears 100% does the abrasive material cause significantly greater wear. One should seek the rationale behind the above observation in the potential interactions be-tween the hard particles of the abrasive material (crushed quartz grains) and the relatively soft cement or carbonaceous inclusions.

As implied by the figures showing the steel surface affected by sand grains, processes of intense abrasion caused by hard mineral grains take place while the material is wearing away (Figure 21). Meanwhile, these grains are subject to comminution, and yet such particles of reduced size continue to abrade the steel sur-face and generate wear products, i.e. loosened fragments of steel. The surface deterioration processes ob-served in all the sandstones containing hematite-based cement or carbon inclusions besides quartz grains proceed differently compared to the cases where quartz sand alone is present.

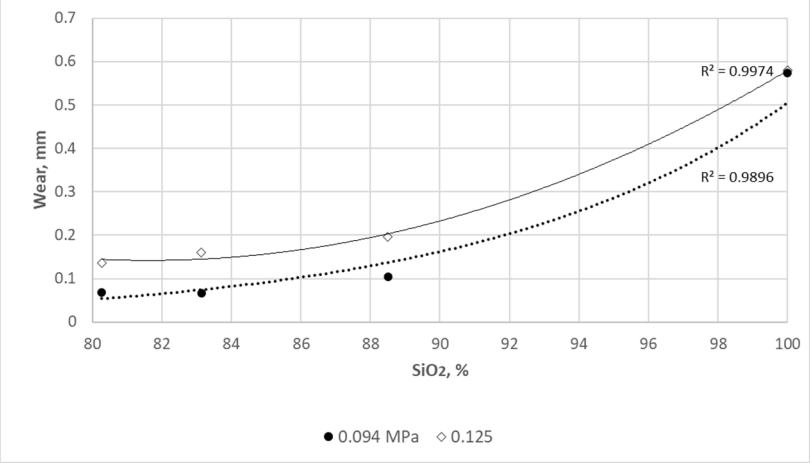

Figure 22. Curves of final mass decrement (WM) of wear-resistant steel in a function of content of quartz in the sand-stone varieties examined and of quartz sand (behaviour established for the loads of 0.094 MPa and 0.125 MPa).

First and foremost, the grains of the minerals which build sandstone become comminuted and subsequently mixed. At the same time, two different processes take place. On the one hand, during the relative motion of the surface of the sam-ples, the steel surface is being abraded by sandstone grain fragments, forming metallic wear products (process accompanied by continuous grain comminution), and on the other hand, the aforementioned mo-tion of the surface of the samples causes the soft components (e.g. hematite cement or carbonaceous inclu-sions) to separate, which leads to the formation of discontinuous layers on the steel surface. As a conse-quence of the effect of quartz grains, they are driven into the surface either directly or through the cement layer previously formed or through inclusions. The embedment of grains in the surface is facilitated by the formation of cement-filled cavities into which the former are pressed under the pressure of the upper sam-ple, the outcome of which is a partial change in the form of abrasive wear from the three-body to the two-body type. The latter form is characterised by a lower intensity of wear compared to the former [9,11].

 doi:10.20944/preprints202405.1730.v1

The loosened wear products along with non-embedded grain fragments may be subject to further commi-nution, or they can continue to cut the mating surfaces as well as break into the dynamically developing discontinuous layer of cement and inclusions, thus becoming inactive.

Based on the studies conducted by the authors, a model of wear of wear-resistant steel in the presence of sandstone grains has been proposed (Figure 23).

The wear model envisages four-stage steel surface deterioration process:

Stage I: Initial condition – non-comminuted quartz grains placed in the test head.

Stage II: initial cutting of the steel surface by comminuted and non-comminuted mineral grain, and initial compaction of the cement and inclusions under the effect of load and relative motion of the samples.

Stage III: further cutting by grains and simultaneous formation of layers of soft sandstone components, facilitated by the temperature increase on the surface of the samples.

Stage IV: further filling of cavities by cement films, formation of pockets capturing larger quartz grains, and inactivation of small grain fragments and wear products by cement films.

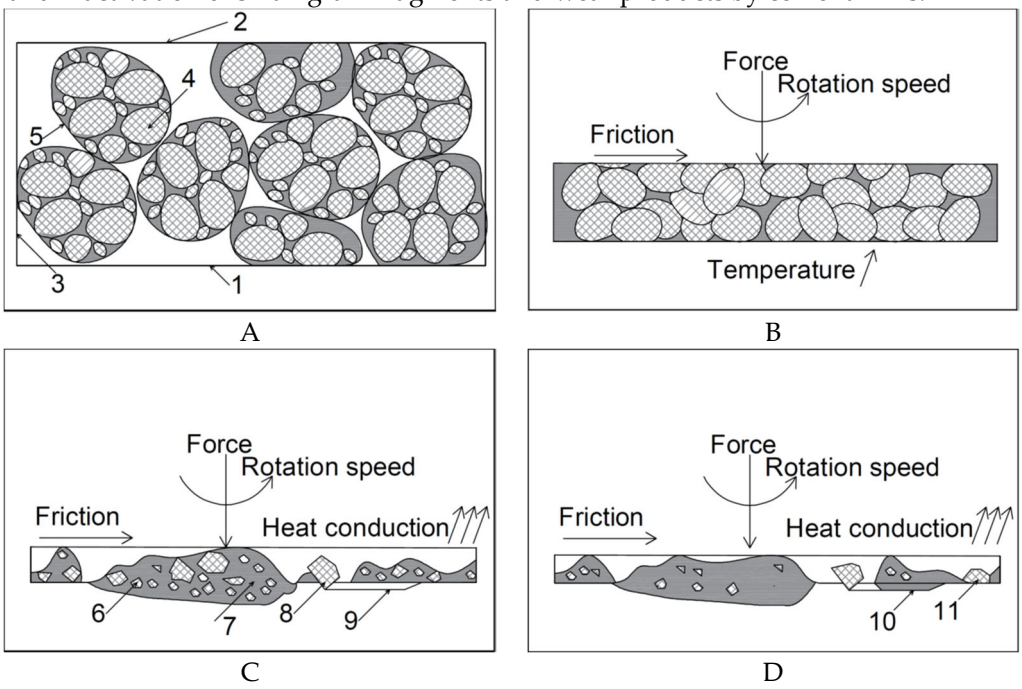

Figure 23. Model of wear in the presence of sandstone, developed for the sample/counter-sample system studied: A – Stage I, B – Stage II, C – Stage III, D – Stage IV; designations: 1 – bottom sample, 2 – top sample, 3 – lateral test head surface, 4 – hard fractions in sandstone (quartz), 5 – cement and inclusions in sandstone, 6 – fragments of grain and wear products, 7 – discontinuous layer of cement and inclusions, 8 – grain frag-ment driven directly into the surface, 9 – scratch on the sample surface, 10 – scratch filled with cement film, 11 – grain fragment driven into the surface and embedded in a pocket.

In the wear model presented above, the hard sandstone fractions are the wear intensifying factors, and their effects are as follows:

- surface abrasion by hard mineral grains and wear products,
- capacity for the formation of extensive surface cracks between abrasion areas as a consequence of aggregate accumulation in surface cracking areas.

On the other hand, the material-forming fractions can mitigate the wear process to some extent by:

- facilitating the settling of mineral abrasive grains in surface damage areas and partially converting the three-body form of abrasive wear into two-body abrasive wear;
- enabling limited capture of hard abrasive particles by discontinuous cement films;
- limiting oxygen access to the loosened steel surface fragments via consolidated cement fractions.

 doi:10.20944/preprints202405.1730.v1

5. Conclusions

Based on the studies conducted by the authors, the following findings have been reached:

1. The form of damage to mating surfaces depends on the type of the abrasive material introduced between them:

– as for the abrasive material based on quartz sand, micro-scratching was found to be the primary steel damage mechanism, the secondary one being the smoothing effect of highly comminuted wear products,

– as for the sandstone-based abrasive, signs of abrasion of the steel surface by grain fragments as well as formation of films comprising minerals forming the sandstone cement (clayey minerals, hematite) and carbonaceous substance were observed.

2. What could also be noticed in the sandstones was the deposition of hard grains, mainly of quartz, in the damaged surface areas, which was facilitated by the presence of soft cement-building minerals (clayey minerals, hematite) and, in the case of Carboniferous sandstone, the presence of carbonaceous matter inclusions.

3. On the surfaces worn in the presence of sandstones, discontinuous and irregular films of cement and carbonaceous inclusions were formed under load.

4. The following conclusions have been drawn with reference to the volumetric wear values measured:

– the most extensive wear was observed in the presence of hard mineral abrasives (quartz sand),

– the wear values obtained for wear-resistant steels in the presence of all the three sandstone varieties studies were very similar to one another.

5. Additionally, models of wear in the presence of sandstone-based abrasive material have been provided in the paper.

In conveyors intended for use in mining workings, wear-resistant steels are supplied according to the specifications of the users of these machines. As a rule, they require a steel surface hardness of not less than 400 HB. Based on the presented results, it is recommended to increase the surface hardness to the range of 475 - 505 HB while maintaining the weldability of the sheets used. The increased cost of purchasing sheets of increased hardness should be returned in the form of an increase in the failure-free operation time of wear-resistant steels.

Author Contributions: Conceptualization, A.N.W. and I.J.; methodology, A.N.W.; investigation A.N.W, A.G., M.K. and A.P.; formal analysis, I.J., A.G. and M.S.; resources, K.M., F.K., M.K. and A.P.; Writing—Original draft preparation, A.N.W. and I.J.; Writing—Review and Editing, K.F. and M.S.; funding acquisition, A.N.W. and K.F. All authors have read and agreed to the published version of the manuscript.

Funding: The article was written as part of the research work of the Department of Mining Mechanization and Robotization of the Silesian University of Technology No. 06/020/BK_21/0052 under the title "Identification of the mechanisms of the impact of abrasive on the basis of sedimentary rocks accompanying coal seams on the surface of friction nodes".

Institutional Review Board Statement: Not applicable.

Informed Consent Statement: Not applicable.

Data Availability Statement: Not applicable.

Conflicts of Interest: The authors declare no conflict of interest.

References

1. Kotwica, K. Zagrożenia generowane podczas mechanicznego urabiania skał zwięzłych – możliwości ich eliminacji lub ograniczenia. *Napędy i Sterowanie* **2018**, *20*, 74-83.
2. Thuro, K. Geologisch-felsmechanische Grundlagen der Gebirgslösung im Tunnelbau. Habilitationsschrift, TU: Munchen, Germany, 2002.

3. Kotwica, K.; Klich A. *Maszyny i urządzenia do drążenia wyrobisk korytarzowych i tunelowych*. Wydawnictwo: ITG KOMAG: Gliwice, Poland, 2011.
4. Wieczorek, A.N. Operation-oriented studies on wear properties of surface-hardened alloy cast steels used in mining in the conditions of the combined action of dynamic forces and an abrasive material. *Arch. Metall. Mater.* **2017**, *62*, 2381–2389.
5. Myszka, D.; Wieczorek, A.N. Effect of phenomena accompanying wear in dry corundum abrasive on the properties and microstructure of austempered ductile iron with different chemical composition. *Arch. Metall. Mater.* **2015**, *60*, 483–490.
6. Hawk, J.A.; Wilson, R.D. Tribology of Earthmoving, Mining, and Minerals Processing. In *Modern Tribology* Handbook; Bhushan, B., Ed.; CRC Press LLC: Boca Raton, FL, USA, 2001; Volume 35.
7. Płaza, S.; Margielewski, L.; Celichowski, G. *Wstęp do tribologii i tribochemia*. Wydawnictwo: Uniwersytetu Łódzkiego: Łódź, Poland, 2005.
8. Tylczak, J.H. Abrasive wear. In *ASM Handbook—Friction, Lubrication, and Wear Technology*; ASM International: Almere, The Netherlands, 1992; Volume 18, 184–190.
9. Stachowiak, G.; Andrew, W. Batchelor. *Engineering tribology*. Butterworth-heinemann, 2013.
10. Zum Gahr, K.H. *Microstructure and Wear of Materials*. Tribology Series Elsevier, The Netherlands, 1987.
11. Stachowiak, G.B.; Stachowiak, G.W. The effects of particle characteristics on three-body abrasive wear. *Wear* **2001**, 249, 201–207.
12. Labaš, M.; Krepelka, F.; Ivaničová, L. Assessment of abrasiveness for research of rock cutting. *Acta Montan. Slovaca* **2012**, *17*, 65–73.
13. Xia, R.; Li, B.; Wang, X.; Yang, Z.; Liu, L. Screening the Main Factors Affecting the Wear of the Scraper Conveyor Chute Using the Plackett–Burman Method. *Hindawi Math. Probl. Eng.* **2019**, 1204091.
14. Wieczorek, A.N. The role of operational factors in shaping of wear properties of alloyed Austempered Ductile Iron. Part II. An assessment of the cumulative effect of abrasives processes and the dynamic activity on the wear property of Ausferritic Ductile Iron. *Arch. Metall. Mater.* **2014**, *59*, 1675–1683.
15. Tlotleng, M.T. Coal Characteristics that Lead to Abrasion during Grinding. Master's Thesis, University of the Witwatersrand, Johannesburg, South Africa, 2011.
16. Ratia, V.; Heino, V.; Valtonen, K.; Vippola, M.; Kemppainen, A.; Siitonen, P.; Kuokkala, V.T. Effect of abrasive properties on the high-stress three-body abrasion of steels and hard metals. *TRIBOLOGIA Finn. J. Tribol.* **2014**, *32*, 3–18.
17. Valtonen, K.; Ratia, V.; Ojala, N.; Kuokkala V.-T. Comparison of laboratory wear test results with the in-service performance of cutting edges of loader buckets. *Wear* **2017**, *388–389*, 93-100.
18. Hakami, F.; Pramanik, A.; Basak, A.K. Effect of the Abrasive Particle Size. In: *Tribology of Elastomers.* Springer Briefs in Applied Sciences and Technology, Springer, Singapore, 2022.
19. Lawrowski, Z. *Tribologia. Tarcie, zużycie i smarowanie*, PWN: Warszawa, Poland, 1993.
20. Mucha, K. Ścierność skał w aspekcie prognozowania zużycia noży kombajnowych. Praca doktorska, AGH University of Science and Technology, Kraków, 2019.
21. Geological digressions: https://www.geological-digressions.com/classification-of-sandstones (accessed on 12 February 2022).
22. Kozłowski, S. *Surowce skalne Polski*. Wydawnictwa Geologiczne: Warszawa, Poland, 1986.
23. https://mineralseducationcoalition.org/minerals-database/sandstone/ (accessed on 29 Juni 2023).
24. https://www.britannica.com/science/sedimentary-rock/Sedimentary-rock-types (accessed on 29 Juni 2023).
25. Garzanti, E. Petrographic classification of sand and sandstone. Earth-Science Reviews 2019, 19, 545–563.
26. Folk, R.L. Petrology of sedimentary rock. Hemphill's.: Austin, Texas, USA, 1968.
27. Pettijohn, F.J.; Potter, P.E.; Siever, R. Sand and sandstone. Springer-Verlag: New York, USA, 1972.
28. Song, Z.; Konietzky, H.; Wu, Y.; Du, K.; Cai X. Mechanical behaviour of medium-grained sandstones exposed to differential cyclic loading with distinct loading and unloading rates. J Rock Mech Geotech. 2022, 14, 1849-1871.
29. Bagde, N.; Petroš, V. Fatigue properties of intact sandstone samples subjected to dynamic uniaxial cyclical loading. Int J Rock Mech Min. 2005, 42, 237–250.
30. Bagde, M.N.; Petroš, V. Waveform Effect on Fatigue Properties of Intact Sandstone in Uniaxial Cyclical Loading. *Rock Mech. Rock Engng.* **2005**, *38*, 169–196.
31. Bagde, M.N.; Petroš, V. The effect of machine behaviour and mechanical properties of intact sandstone under static and dynamic uniaxial cyclic loading. *Rock Mech Rock Eng* **2005**, *38*, 59–67.
32. Song, H.; Zhang, H.; Kang, Y.; Huang, G.; Fu, D.; Qu, C. Damage evolution study of sandstone by cyclic uniaxial test and digital image correlation. *Tectonophysics* **2013**, *608*, 1343–1348.
33. Xin, C.; Zilong, Z.; Lihai, T.; Haizhi, Z.; Zhengyang, S. Fracture behavior and damage mechanisms of sandstone subjected to wetting-drying cycles. *Engineering Fracture Mechanics* **2020**, *234*, 107109.
34. Zhao, Y.; Zhou, H.; Zhong, J. Study on the relation between damage and permeability of sandstone at depth under cyclic loading. *Int J Coal Sci Technol* **2019**, *6*, 479–492.

35. Vaneghi, R.G.; Ferdosi, B.; Okoth, A.D.; Kuek, B. Strength degradation of sandstone and granodiorite under uniaxial cyclic loading, *J Rock Mech Geotech.* **2018**, *10*, 117–126.
36. Yang, S.Q.; Ranjith, P.G.; Huang, Y.H.; Yin, P.F.; Jing, H.W.; Gui, Y.L.; Yu, Q.L. Experimental investigation on mechanical damage characteristics of sandstone under triaxial cyclic loading. *Geophysical Journal International* **2015**, *201*, 662–682.
37. Yang, S.Q.; Jing, H.W. Evaluation on strength and deformation behavior of red sandstone under simple and complex loading paths. *Engineering Geology* **2013**, *164*, 1–17.
38. Yang, S.Q.; Jing, H.W.; Wang, S.Y. Experimental investigation on the strength, deformability, failure behavior and acoustic emission locations of red sandstone under triaxial compression. *Rock Mech Rock Eng* **2012**, *45*, 583–606.
39. Zhao, G.F.; Russell, A.R.; Zhao, X.; Khalili, N. Strain rate dependency of uniaxial tensile strength in Gosford sandstone by the Distinct Lattice Spring Model with X-ray micro CT. *Int J Solids Struct* **2014**, *51*, 1587–1600.
40. Liu, E.; He, S. Effects of cyclic dynamic loading on the mechanical properties of intact rock samples under confining pressure conditions, *Engineering Geology* **2012**, *125*, 81–91.
41. Ray, S.K; Sarkar, M.; Singh, T.N. Effect of cyclic loading and strain rate on the mechanical behaviour of sandstone, *International Journal of Rock Mech. Rock Eng*. **1999**, *36*, 543–549.
42. Feng, X.T.; Chen, S.; Zhou, H. Real-time computerized tomography (CT) experiments on sandstone damage evolution during triaxial compression with chemical corrosion. *International Journal of Rock Mech. Rock Eng*. **2004**, *41*, 181–192.
43. Figarska-Warchoł, B.; Rembi´s, M. Lamination and Its Impact on the Physical and Mechanical Properties of the Permian and Triassic Terrestrial Sandstones. *Resources* **2021**, *10*, 42.
44. Li, Z.; Zhu, Y.; Song, Q.; Wang, P.; Liu, D. Dynamic Mechanical Properties and Failure Characteristics of Sandstone with Pre-Flaws Parallel to the Loading Direction. *Sustainability* **2023**, *15*, 3587.
45. Strzałkowski, P.; Kaźmierczak, U.; Wolny, M. Assessment of the method for abrasion resistance determination of sandstones on Böhme abrasion test apparatus. *Bull Eng Geol Environ* **2020**, *79*, 4947–4956.
46. Zhao, G.; Wang, L.; Zhao, N.; Yang, J.; Li, X. Analysis of the Variation of Friction Coefficient of Sandstone Joint in Sliding. *Adv Struct Eng* **2020** | Article ID 8863960 | https://doi.org/10.1155/2020/8863960.
47. Mucha, K. Application of Rock Abrasiveness and Rock Abrasivity Test Methods—A Review. *Sustainability* **2023**, *15*, 11243.
48. Jonczy, I.; Mucha, K. Relationships between the Petrographic and Abrasive Properties of Sandstones in the Aspect of Their Cutting. *Energies* **2022**, *15*, 2692.
49. Tang, S.-H.; Zhang, X.-P.; Liu, Q.-S.; Xie,W.-Q.; Wang, H.-J.; Li, X.-F.; Zhang, X.-Y. New soil abrasion testing method for evaluating the influence of geological parameters of abrasive sandy ground on scraper wear in TBM tunnelling. *Tunn. Undergr. Space Technol.* **2022**, *128*, 104604.
50. Abu Bakar, M.; Majeed, Y.; Rostami, J. Influence of moisture content on the LCPC test results and its implications on tool wear in mechanized tunneling. *Tunn. Undergr. Space Technol*. **2018**, *81*, 165–175.
51. Terva, J.; Teeri, T.; Kuokkala, V.-T.; Siitonen, P.; Liimatainen, J. Abrasive wear of steel against gravel with different rock–steel combinations. *Wear* **2009**, *267*, 1821–1831.
52. Yarali, O.; Yasar, E.; Bacak, G.; Ranjith, P.G. A study of rock abrasivity and tool wear in Coal Measures Rocks. *Int. J. Coal Geol.* **2008**, *74*, 53–66.
53. Barzegari, G.; Uromeihy, A.; Zhao, J. Parametric study of soil abrasivity for predicting wear issue in TBM tunneling projects, *Tunn. Undergr. Sp. Technol. Inc. Trenchless Technol. Res.* **2015**, *48*, 43–57.
54. Jakobsen, P.D.; Lohne, J. Challenges of methods and approaches for estimating soil abrasivity in soft ground TBM tunnelling, *Wear*. **2013**, *308*, 166–173.
55. Konat, Ł. Struktury i właściwości stali Hardox a ich możliwości aplikacyjne w warunkach zużywania ściernego i obciążeń dynamicznych. Dissertation, Politechnika Wrocławska, Wrocław, 2007.
56. Hardox – Das Verschleißblech der vielen Möglichkeiten. SSAB: Oxelösund, Sweden, 2002.
57. Dudziński, W.; Konat, Ł.; Pękalska, L.; Pękalski, G. Struktury i właściwości stali Hardox 400 i 500. *Inżynieria Materiałowa* **2006**, *151*, 139–142.
58. Shi, Z.; Zhu, Z. Case study: Wear analysis of the middle plate of a heavy-load scraper conveyor chute under a range of operating conditions. *Wear* **2017,** *380-381*, 36–41.
59. Wang, S.; Ge, Q.; Wang, J. The impact wear-resistance enhancement mechanism of medium manganese steel and its applications in mining machines. *Wear* **2017**, *376-377*, 1097–1104.
60. Heino, V. The Effect of Rock Properties on the High Stress Abrasive Wear Behavior of Steels, Hardmetals and White Cast Irons. Dissertation, Tampere University of Technology. Publication 1575, Tampere, 2018.
61. Haiko, O.; Somani, M.; Porter, D.; Kantanen, P.; Kömi, J.; Ojala, N.; Heino, V. Comparison of impact-abrasive wear characteristics and performance of direct quenched (DQ) and direct quenched and partitioned (DQ&P) steels, *Wear* **2017**, 400–401.
62. Ojala, N.; Valtonen, K.; Heino, V.; Kallio, M.; Aaltonen, J.; Siitonen, P.; Kuokkala, V.-T. Effects of composition and microstructure on the abrasive wear performance of quenched wear resistant steels, *Wear* **2014**, 317.

 doi:10.20944/preprints202405.1730.v1

63. Thakare, M.R.; Wharton, J.A.; Wood, R.J.K.; Menger, C. Effect of abrasive particle size and the influence of microstructure on the wear mechanisms in wear-resistant materials, *Wear* **2012**, *276–277*, 16–28.
64. Michalczewski, R.; Kalbarczyk, M.; Mańkowska-Snopczyńska, A.; Osuch-Słomka, E.; Piekoszewski, W.; Snarski-Adamski, A.; Szczerek, M.; Tuszyński, W.; Wulczyński, J.; Wieczorek, A. The Effect of a Gear Oil on Abrasion, Scuffing, and Pitting of the DLC-Coated 18CrNiMo7-6 Steel. *Coatings* **2019**, *9*, 2.
65. Jonczy, I.; Wieczorek, A.N.; Podwórny, J.; Gerle, A.; Staszuk, M.; Szweblik, J. Characteristics of hard coal and its mixtures with water subjected to friction. *Gospod. Surowcami Miner. Miner. Resour. Manag.* **2020**, *36*, 185–201.
66. Jonczy, I.; Wieczorek, A.; Filipowicz, K.; Mucha, K.; Kuczaj, M.; Pawlikowski, A.; Nuckowski, P.; Pieczora, E. Carboniferous Clays on Surfaces of Friction Nodes. *Energies*. **2021**; *14*, 1422.
67. Wieczorek, A.N.; Jonczy, I.; Bala, P.; Stankiewicz, K.; Staszuk, M. Testing the Wear Mechanisms of the Components of Machines Used in Fossil Energy Resource Extraction. *Energies* **2021**, *14*, 1–20.
68. Wieczorek, A.N.; Jonczy, I.; Filipowicz, K.; Kuczaj, M.; Pawlikowski, A.; Łukowiec, D.; Staszuk, M.; Gerle, A. Study of the Impact of Coals and Claystones on Wear-Resistant Steels. *Materials* **2023**, *16*, 2136.
69. Hawk, J.A.; Wilson R.D. Tribology of Earthmoving, Mining, and Minerals Processing, in: *Modern Tribology Handbook* (editor in chief B. Bhushan). CRC Press LLC., 2001, Volume 35.
70. Wieczorek, A.N.; Polis, W. Operation-oriented method for testing the abrasive wear of mining chain wheels in the conditions of the combined action of destructive factors. *Manag. Syst. Prod. Eng.* **2015**, *19*, 175–178.
71. Norman, T.E. Wear in ore processing machinery. In: *Wear Control Handbook*; Peterson, M.B.; Winer, W.O., Eds.; ASME: New York, USA, 1980, pp. 1009–1051.
72. Scott, D. Wear. In: Industrial tribology - The practical aspects of friction, lubrication and wear, Elsevier 1983, pp. 12–30.
73. Szczerek, M.; Wiśniewski, M. *Tribologia i tribotechnika*. Polskie Towarzystwo Tribologiczne, Instytut Technologii Eksploatacji, Stowarzyszenie Inżynierów i Techników mechaników Polskich: Radom, Poland, 2000, pp. 15–19.